Published in final edited form as:
Carbohydr Res. 2011 November 8; 346(15): 2499–2510. doi:10.1016/j.carres.2011.08.031.

NMR and conformational studies of linear and cyclic oligo-(1→6)-β-D-glucosamines

Alexey A. Grachev[a], **Alexey G. Gerbst**[a], **Marina L. Gening**[a], **Denis V. Titov**[a], **Olga N. Yudina**[a], **Yury E. Tsvetkov**[a], **Alexander S. Shashkov**[b], **Gerald B. Pier**[c], and **Nikolay E. Nifantiev**[a,*]

[a]Laboratory of Glycoconjugate Chemistry, N. D. Zelinsky Institute of Organic Chemistry Russian Academy of Sciences, Leninsky prospect 47, 119991 Moscow (Russia)

[b]NMR spectroscopy, N. D. Zelinsky Institute of Organic Chemistry Russian Academy of Sciences, Leninsky prospect 47, 119991 Moscow (Russia)

[c]Channing Laboratory, Brigham and Women's Hospital, Harvard Medical School, 181 Longwood Avenue, Boston, MA (USA)

Abstract

The conformational behavior of a series of linear and cyclic oligo-(1→6)-β-D-glucosamines and their N-acetylated derivatives, which are related to fragments of natural poly-N-acetylglucosamine, was studied by theoretical molecular modeling and experimental determination of transglycosidic vicinal coupling constants $^{3}J_{C,H}$ and $^{3}J_{H,H}$. Molecular dynamics simulations were performed under several types of conditions varying in the consideration of ionization of amino groups, solvent effect and temperature. Neural network clustering and asphericity calculations were performed on the basis of molecular dynamics data. It was shown that disaccharide fragments in the studied linear oligosaccharides were not rigid, and tended to have several conformers, thus determining the overall twisted shape with helical elements. In addition, it was found that the behavior of C5–C6 bond depended significantly upon the simulation conditions. The cyclic di-, tri-, and tetrasaccharides mostly had symmetrical ring-shaped conformations. The larger cycles tended to adopt more complicated shapes, and the conformational behavior of their disaccharide fragments was close to that in the linear oligosaccharides.

Keywords

Cyclic oligosaccharides; Glucosamine; Conformation analysis; MM3; SASA; Transglycosidic coupling constants

*Corresponding author. Tel./fax: +7 499 135 8784. nen@ioc.ac.ru (N.E. Nifantiev).

Supplementary data

Supplementary data associated with this article can be found, in the online version, at doi:.....

1. Introduction

Poly-N-acetylglucosamine (PNAG) represents the core component of biofilms formed by *Staphylococcus aureus*[1] and other pathogens.[2–6] Biofilms are important for bacterial virulence and environmental survival. The elucidation of PNAG's secondary structure may help understand the organization of the whole biofilm and possible means to disrupt it to reduce the consequences of bacterial infections. Therefore, determination of the conformational properties of PNAG and its oligosaccharide fragments is an important goal in the chemistry of natural compounds.

In this article we report on the results of NMR and theoretical conformational investigations of a large group of synthetic oligosaccharides related to the fragments of PNAG. These are linear **1a–6a** and cyclic **7a–12a** (Fig. 1) oligoglucosamines and their corresponding N-acetylated derivatives **1b–12b**. Synthesis of these compounds has been described[7–9] and some of them have been documented to induce formation of protective antibodies in animals when conjugated to carrier proteins.[10] These oligosaccharides differ from each other by a number of structural factors such as the presence of N-acetyl groups, cyclization and elongation of the oligosaccharide chains which may drastically influence the biological activity in relation to biofilm formation and vaccine potential.[10] The conformational analysis of oligosaccharides was based on the comparison of homo- ($^3J_{H,H}$) and heteronuclear ($^3J_{C,H}$) spin-spin coupling constants (SSCC) experimentally measured by NMR and calculated by Karplus equations using data from molecular dynamic (MD) simulations. This approach previously gave good results for elucidation of the conformations of a number of oligosaccharide groups related to natural polysaccharides.[11,12]

Preliminary results from the conformational study of the cyclic glucosamines was reported previously;[9] herein these compounds are investigated in more detail and in comparison with corresponding linear oligosaccharides. Their study is of special interest due to the structural relationship between cycloglucosamines and cyclodextrins. The latter are widely known for the ability to form inclusion complexes with various compounds.[13] The presence of amino groups along with the central cavity in the studied oligosaccharides provides the possibility to modify and possibly extend their ability to form complex structures. Apart from our own previous publication[9], only one work[14] is known to us that describes the conformational analysis of (1→6)-linked oligosaccharides that consist of three or more monosaccharide residues.

2. Results and Discussion

2.1. NMR Spectroscopy Study

The structures of the synthesized oligoglucosamines **1a,b–4a,b** and **6a,b–12a,b** were determined by various NMR spectroscopy techniques (hexasaccharides **5a** and **5b** were not synthesized). Particularly, the NMR investigation included analysis of one-dimensional ^1H and ^{13}C and two-dimensional homonuclear $^1H/^1H$ COSY, TOCSY, NOESY and ROESY and heteronuclear $^1H/^{13}C$ HSQC, HSQC-TOCSY and HMBC spectra for solutions of the compounds in D_2O. Analysis of COSY and TOCSY spectra permitted us to assign signals for protons in coupled spin systems of monosaccharide residues in ^1H NMR spectra (Table 1). Analysis of 2D heteronuclear spectra HSQC and HSQC-TOCSY led to the assignment of all signals in one-dimensional ^{13}C NMR spectra (Table 2) based on the ^1H chemical shifts thus completing the analysis of monomeric compositions of the oligoglucosamines. The sequence of monosaccharide units in oligosaccharide chains is traditionally determined by the analysis of the nuclear Overhauser effect (NOE) values between pairs of protons in neighboring monosaccharide units. The values of the Overhauser effects were measured by means of NOE and ROE NMR experiments. However, for most of the oligoglucosamines

examined in the present work this approach was not applicable due to the overlap of the signals both in 1D and 2D NOE and ROE spectra, as well as to the absolute values of NOE being close to zero in the large oligosaccharides.

NMR experiments based on the observation of inter-unit interactions between hydrogen and carbon atoms linked by long-range SSCCs were used for the determination of monosaccharide sequences in the oligoglucosamines **1a,b–12a,b**. The techniques employed were J-HMBC[15,16] and J-resolved,[17,18] that allowed for the quantitative measurement of SSCC values. The obtained constant values were later used in the conformational analysis of oligoglucosamines **1a,b–12a,b**.

Oligoglucosamines **1a–4a** and **6a–12a** were synthesized as acetic acid salts.[7–9] Analysis of integral intensities in ^{1}H NMR spectra of these compounds showed that in the case of cyclic oligosaccharides **7a–12a** the stoichiometric salts were formed with one molecule of acetic acid per each amino group. In the case of linear di- (**1a**), tri- (**2a**) and tetrasaccharide (**3a**) acetate ions were also present in stoichiometric ratio to amino groups, while in penta- (**4a**) and heptasaccharide (**6a**) only four acetates were present. It was supposed that partial hydrolysis of oligoglucosamine acetic salts occurred in water solution with formation of free amino-groups and some amount of acetic acid evaporated during the sample preparation (pH of resulting solutions was about 5.5). Protonated amino groups in oligosaccharides **1a–4a** and **6a–12a** were randomly distributed and protons may exchange the positions between them.

The introduction of N-acetyl groups into the oligoglucosamines was accompanied by significant changes in chemical shift values (Tables 1–4). In ^{1}H NMR spectra, chemical shifts of protons H-2 in glucosamine residues, which were directly connected to C-2 (α-carbons) bearing amino groups, were affected most greatly (the average value of Δδ(H-2) was 0.67 ppm; spectral N-acetylation effects are given in Supplementary Materials). The effects on β-protons (H-1 and H-3) were considerably smaller (the average values of Δδ(H-1) and Δδ(H-3) were −0.19 and −0.09 ppm, respectively). The effects on other protons of glucosamine residues were also small. Analysis of ^{13}C NMR spectra showed that chemical shifts of α-carbons (C-2) did not change upon N-acetylation. In this case the biggest effects were observed on β-carbons (C-1 and C-3), the average values of Δδ(C-1) and Δδ(C-3) being 2.0 ppm and 1.7 ppm, correspondingly.

The comparison of the ^{1}H and ^{13}C spectra of linear N-acetylated oligoglucosamines **1b–6b** showed that all monosaccharide residues in these molecules could be divided into three groups according to the characteristic features in their ^{1}H and ^{13}C chemical shifts (Tables 1 and 2). These were terminal residues at the non-reducing ends, middle residues and the residues at the reducing ends. All middle residues regardless of the length of oligosaccharide chain had very close chemical shifts.

^{1}H and ^{13}C spectra of cyclic N-acetylated oligoglucosamines **7b–12b** contained a set of signals corresponding to a single monosaccharide residue (Tables 3 and 4) indicating that conformational states of all monosaccharide residues within a molecule were averaged during molecular motion. In the case of small cycles (di-, tri-, and tetrasacharide **7b–9b**) the chemical shifts changed significantly upon the cycle enlargement, but in the case of larger cycles (penta-, hexa-, and heptasaccharide **10b–12b**) they were not affected by the change of the molecular size and became close to those in internal units of linear oligoglucosamines **2b–4b, 6b** (Tables 1 and 2).

In oligoglucosamines **1a–4a** and **6a–12a** the tendencies in chemical shift values were almost the same as in the case of N-acetylated oligosaccharides **1b–4b** and **6b–12b** (Tables 1–4, Fig. 2). The only exception were linear disaccharide **1a** and heptasaccharide **6a**, where the

chemical shifts of C-1 and C-3 (β-carbons relative to amino groups) differed from those in tri- **(2a**), tetra- (**3a**) and pentasaccharide **4a**. Most likely this difference in chemical shifts is explained by the difference in ionization and solvation of oligosaccharides that was discussed above.

Conformations of pyranoside rings in common carbohydrates change only slightly during molecular motion and are considered to have little influence on the conformational changes of the whole saccharide molecule.[19,20] This also applied to most of the oligoglucosamines in this investigation as confirmed by the large values of intra-unit vicinal constants $^{3}J_{H,H}$ shown in Supplementary Materials, that obviously corresponded to glucopyranose residues in $^{4}C_{1}$ conformation.[19] The only exception were cyclic disaccharides **7a** and **7b**, where the coupling constants $^{3}J_{H,H}$ within the glucosamine residues had values atypical for the $^{4}C_{1}$ conformation (Table 3 in Supplementary Materials). This could be explained by conformational distortions of the pyranose rings in these compounds occurring due to their strained structure.[9] Similar distortions had already been observed for cyclogentiobioside.[21,22]

Spatial structures of (1→6)-linked pyranosides are primarily determined by the conformations of glycosidic bonds between monosaccharide residues which are described in terms of dihedral angles φ, ψ, and ω (Fig. 3). The values of these angles are connected with experimentally measured values of $^{3}J_{C,H}$ and $^{3}J_{H,H}$ coupling constants around the glycosidic linkages through the Karplus equations[23,24] (Fig. 3). Hence, to investigate the conformational properties of oligoglucosamines **1a,b–4a,b** and **6a,b–12a,b**, the experimental values of transglycosidic constants $^{3}J_{C,H}$ and $^{3}J_{H,H}$. were analyzed

J-HMBC[15,16] is one of the most powerful methods for the detection of long-range carbon-proton SSCCs ($^{n}J_{C,H}$, where n≥2). This experiment was used to determine the values of constants Jψ (Fig. 3) in the studied oligoglucosamines. However, the determination of constants Jφ by J-HMBC experiment was not always possible due to the overlap of the correlation peaks in the spectra. Therefore, a selective 2D J-resolved[17,18] experiment was employed for the determination of Jφ in these cases. The detailed description of the NMR technique for the measurement of transglycosidic coupling constants $^{3}J_{C,H}$ in oligosaccharides was provided in our previous work[11] and can also be found in the experimental section of this article. The values of $^{3}J_{H,H}$ (Jω**R** и Jω**S**, Fig. 3) were measured directly from one-dimensional ^{1}H NMR spectra as the difference between peak maxima in multiplets. Many of the Jω constants in the studied oligoglucosamines had small values, not exceeding 2 Hz (Tables 5 and 6). Their precise determination by the direct measurement as described above was impossible due to the influence of signal shapes of all multiplet components on the whole multiplet shape. The bigger value of the multiplet component width drastically increases the error during Jω measurement, which in some cases may reach 70%. Therefore, the full line shape analysis approach was used[25] for the determination of small constants. Unfortunately, it was still impossible to measure $^{3}J_{C,H}$ and $^{3}J_{H,H}$ constants in linear penta- (**4a** and **4b**) and heptasaccharides (**6a** and **6b**) due to the strong overlap of signals.

Analysis of the available experimental values for constants measured for linear oligoglucosamines **1a–3a** revealed that they did not depend neither upon the oligosaccharide chain length nor the position of a linkage in the chain, contrary to the case in the previously studied β-(1→3)-linked oligofucosides.[12] For cyclic structures with more than five residues **10a–12a** SSCCs showed the same tendency, and their absolute values were close to those in linear molecules **1a–3a**; the difference between the corresponding constants did not exceed 1.2 Hz. In small cyclic molecules **7a–9a**, however, SSCCs changed considerably upon the enlargement of the molecule (Table 6). This indicated that the dominating conformations of

glycosidic linkages in these cycles differed greatly from those in the cyclic penta-, hexa- and heptasaccharides.[9] Similar conclusions could be achieved during the analysis of ^{1}H and ^{13}C chemical shifts (Tables 1–4). Changes in the spectra occurred because chemical shifts in carbohydrates are peculiarly dependent on the conformations of these molecules.[26]

In case of N-acetylated derivatives **1b–4b** and **6b–12b** the $^{3}J_{C,H}$ and $^{3}J_{H,H}$ values were generally similar to those of the corresponding fragments in free amines **1a–4a** and **6a–12a**. The exception was observed in the case of Jφ constants in the linear molecules, which in **1b–3b** slightly exceeded the corresponding SSCC values in **1a–3a** (Table 5).

2.2. Molecular Modeling

To elucidate conformational properties of glucosamines **1a,b–12a,b**, molecular dynamics (MD) calculations were performed. They were carried out using MM3 force field (TINKER program suit). Although the MM3 was originally developed as a general purpose force field, it is now known to reproduce structural characteristics of carbohydrates among other parameter sets.[27,28]

One problem that arose during the studies of oligoglucosamines **1a–12a** was the possibility of the dissociation of the ammonium salts with the formation of free amines. Therefore MD calculations for these molecules were carried out both for ammonium model ($-NH_3^+$) and deprotonated amine model ($-NH_2$). In the latter case, solvent effects were considered using the continual Solvent Accessible Surface Area model (SASA) and a more rough approach based on the value of dielectric permittivity constant (81 for water). In the case of ammonium salts the SASA model cannot be applied without careful consideration of atomic charges and counter ions which is difficult to carry out on a molecular mechanics level, hence an approach based on the value of the dielectric permittivity constant was used. Both approaches (SASA and dielectric permittivity constant) were tried and compared in the case of N-acetylated oligoglucosamines **1b–12b**. Besides, different temperatures were used to investigate the possibility of crossing internal barriers. Aglycon moieties were not considered in the simulation.

Simulation time was 50 ns for cyclic glucosamines **7a,b–12a,b**. For linear oligosaccharides **1a,b–6a,b**, adiabatic conformational maps were built first using a dihedral driving algorithm for each linkage.[29] After that, several 10 ns trajectories were simulated starting from the global minima found on each map. Snapshot structures were written every 5 ps and then used for further analysis. This yielded 10000 conformations for cyclic oligosaccharides and 2000×N conformations for the linear structures, where N is the number of glycosidic linkages in the molecule.

In the beginning, the calculations were performed at a temperature of 300 K. However, the results obtained for cyclic structures **7a,b–12a,b** were contradictory to the experimental data independently on the solvation model used. In particular, the values of transglycosidic SSCC $^{3}J_{C,H}$ and $^{3}J_{H,H}$ calculated by Karplus equations (Fig. 3) differed strongly from each other across the glycosidic linkages, while experiments showed all linkages to behave equally. For example, in ^{1}H and ^{13}C NMR spectra there were sets of signals corresponding to a single monosaccharide unit.

It was suggested that this problem might arise from the overestimation of conformational barriers in the MM3 calculations which makes the temperature of 300 K insufficient for the molecules to cross all barriers to obtain averaged conformations for each glycosidic linkage. A higher temperature of 700 K provided satisfactory results. The calculated values of constants (700 K) are shown in Table 6 (see also Table 5 in Supplementary Materials).

Alteration of the solvation model both in the case of linear and cyclic structures (Tables 5 and Table 6) mostly influenced the values of proton coupling constants $^3J_{H,H}$ (Jω**R** and Jω**S**) which were determined by the value of ω torsion, while the values of carbon-proton constants $^3J_{C,H}$ (Jφ, Jψ**R** and Jψ**S**) changed by not more than 1 Hz, which is within the experimental accuracy of these SSCC measurement. We explain such behavior by the difference in slopes of Karplus functions for $^3J_{H,H}$ and $^3J_{C,H}$ (Fig. 3) which leads to greater changes of $^3J_{H,H}$ values upon the equal changes in torsions. Besides, the alteration of the solvation model obviously changed the energy difference of rotamers resulting from the rotation of ω torsion.[30] In the case of cyclic oligoglucosamines **7a,b–12a,b** these torsions depended much less upon the solvation model used due to the conformational restrictions.

The comparison of the calculated SSCC values with those measured experimentally for the linear and cyclic oligosaccharides showed good coincidence for heteronuclear constants $^3J_{C,H}$ (for most of them the difference did not exceed 1 Hz). For $^3J_{H,H}$ constants the coincidence was expectedly worse, especially for the linear oligosaccharides **1a,b–6a,b**.

The greatest deviation of the calculated hetero- and homonuclear SSCCs from the experimental ones was observed in the case of cyclic disaccharides **7a** and **7b**. These molecules are very constrained and suffer from monosaccharide ring deformations (see above in the NMR Spectroscopy Study section and Table 3 in the Supplementary Materials), that probably imply some torsional or van-der-Waals interactions unusual for saccharides, which are not considered correctly by molecular mechanics.

We performed the analysis and visualization of the results of molecular modeling, including the torsions values φ, ψ and ω (Fig. 3). In our case almost all molecules contained more than one such a linkage. This required that 3N variables be used to describe the conformation of the whole molecule. Such a huge data array was difficult to visualize directly, hence we employed two approaches for the analysis of MD trajectories. The scatter plots were built for pairs of angles (φ, ψ), (φ, ω) and (ψ, ω) (Fig. 4). Analysis of these plots showed that all disaccharide fragments in the studied oligoglucosamines **1a,b–12a,b** (both linear and cyclic) were characterized by the presence of multiple conformational minima allowing the conclusion that they were not rigid. The scatter plots of linear oligosaccharides within the same coordinates (φ, ψ), (φ, ω) and (ψ, ω) were similar to each other (Fig. 4) for different disaccharide fragments and molecules suggesting the similarity of conformational behavior. In the case of cyclic oligosaccharides **7a,b–12a,b** the number of accessible conformational states was greater than in the linear ones which apparently resulted from the higher temperature (700 K) used during MD simulations of cycles (see above). The areas corresponding to these states in the larger cyclic oligosaccharides were to be found at the scatter plots around points which were close to those corresponding to the linear molecules, but for the small cycles (di-, tri-, and tetrasaccharide) a considerable difference in the positions of conformational minima was observed. It is explained by the restricted flexibility of the small-sized cyclic saccharides, which confirms the observations made during the analysis of experimental chemical shifts and SSCC values. The scatter plots of non-N-acetylated oligoglucosamines **1a–12a** (see Fig. 1 in Supplementary Materials) did not differ significantly from those of their N-acetylated counterparts **1b–12b** (Fig. 4).

The second approach to the analysis of MD data was based on their clustering by means of artificial neural networks (ANN) of ART2 (Adaptive Resonance Theory) topology implemented in the Stuttgart Neural Network Simulator (SNNS v4.2).[31–33] This permitted the analysis of the regions in the conformational space accessible during MD simulations using all three torsions for each linkage. Furthermore, it allowed the analysis of the conformation of the studied molecules as a whole, using all torsions for all linkages. However, this only showed not unexpectedly that each linkage behaved independently,

except for those in small cyclic structures (2–3 units) where MD simulations likely failed to provide all the available conformations due to high rigidity. Therefore we focused on the analysis of separate linkages. The torsional angles were represented in terms of corresponding coupling constants $^3J_{C,H}$ and $^3J_{H,H}$ (Fig. 3). ANN assisted clustering was performed for the MD trajectories obtained without the solvation model with dielectric constant of 81, and for those obtained using SASA model.

Five clusters in the space of (φ, ψ_R, ψ_S) angles were found for every linkage in the linear oligosaccharides, two of them tending to occupy over 70% of the whole array. They were characterized with (φ, ψ_R, ψ_S) torsions being around (40°, −60°, 60°) and (40°, −160°, −55°). It correlated with one or two big clouds to be found on (φ, ψ) scatter plots, which represented two conformers, sometimes without distinct border. Torsional angle ω had preferable values of −60° or +60° independent of the (φ, ψ) values. Conformations corresponding to these clusters are shown in Fig. 5. The molecules constructed from the preferable conformations of glycosidic linkages are characterized by twisted shapes in which the substituents at C-2 mostly protrude into the outer space and did not encounter any spatial hindrances, hence their acetylation did not lead to a considerable conformational change. This explains the similarity between free amines and their N-acetylated counterparts established during NMR investigation (See above in NMR Spectroscopy Study section).

A global minima search was attempted via geometry optimization of the snapshot structures of the linear oligosaccharides. The shape corresponding to the energy minima of the large linear oligosaccharides calculated without taking into account the solvent effects tended to be a right-hand helix (Fig. 6A). Minima found using the SASA model had rather complicated twisted shapes with some helical elements maintained both for the acetylated and free amines (Fig. 6B). This correlated with MD results and suggested that these conformations may be regarded as adequate models of the studied molecules in water solution.

It is noteworthy that the conformers of C5–C6 bond found during the calculations corresponded mainly to *gt* rotamers of ω with comparable amounts of the *gg* rotamer. The amount of the *tg* rotamer was significantly smaller although still observable. Ratios of *gt* and *gg* conformers changed slightly in different disaccharide fragments of the studied molecules. This is contradictory to the general opinion in which the relative weights of these rotamers in (1→6)-linked diglucoside fragment are 29:70:1 (*gt*:*gg*:*tg*).[28]

The large cyclic structures were also characterized by the similar clusters indicating that with increase in the monosaccharide residue number in the cycle, the conformational properties of the disaccharide fragments became similar to those in the linear structures. Thus, the large cyclic oligosaccharides have conformational shapes that can be described as a twisted ring. In the small cycles the number of clusters was less than five and there presented clusters with average values of coupling constants that deviated greatly from those calculated over the whole trajectory. On the whole, the conformations of the small cycles are rather restrained flattened rings.

Another parameter that was used to analyze the behavior of the studied molecules during MD simulation were so called asphericity values,[34] which can be calculated according to formula $A^3/36\pi V^2$, where A – is the molecular surface and V – molecular volume. Bigger values of this parameter indicate a greater deviation of the molecular shape from an ideal sphere. In our study, the distributions of asphericities were calculated over all MD trajectories computed under SASA conditions: the obtained results are presented in Fig. 7. The area under each graph is normalized to an equal value, thus the differences in the broadness of these distributions can be interpreted as the difference in total molecular

flexibility. It can be seen that it increases upon the enlargement of the molecules, both linear and cyclic, but in the latter the increase is dramatic from the di- to the heptasaccharide. This also suggests that the rigidity present in smaller cycles falls upon the increase in the monosaccharide unit quantity and when it reaches the values of 6–7, the conformational behavior of the cyclic oligosaccharides actually becomes similar to that of the linear chains.

In the case of the N-acetylated glucosamines the shapes of the asphericity distributions are similar but their maxima are slightly shifted towards the range of larger values. This supports the finding that the introduction of N-acetates does not affect the whole conformational shape of the studied compounds.

2.3. Conclusions

In this paper we have discussed the conformational properties of linear **1a,b–6a,b** and cyclic **7a,b–12a,b** oligo-(1→6)-β-D-glucosamines investigated by means of NMR spectroscopy and theoretical modeling. The experimental values of homo- ($^3J_{H,H}$) and heteronuclear ($^3J_{C,H}$) SSCC were used to characterize conformational state of the studied oligosaccharides in water solution. They were compared to SSCCs calculated using the data of MD simulations. The simulations were performed under several types of conditions used for the consideration of ionization of free amines, solvent effect and temperature. For cyclic structures **7a,b–12a,b** the obtained results at 300 K were contradictory to the experiment, thus the higher temperature of 700 K was employed leading to an interpretable outcome.

The comparison of the calculated SSCC values with those measured experimentally for linear and cyclic oligosaccharides showed good coincidence for heteronuclear constants $^3J_{C,H}$: in the most cases the difference did not exceed 1 Hz. In the case of homonuclear SSCCs the match between the experimental and the calculated values was worse. It was found that the simulated behavior of the C5–C6 bond depended strongly on the solvation model used, especially for the linear oligosaccharides. For cyclic disaccharides **7a** and **7b** the greatest overall SSCCs mismatch was observed possibly due to high straints and monosaccharide ring deformations, which are not considered correctly by molecular mechanics. On the other hand, experimental study by SSCCs measurement was impossible for some molecules due to the overlaps of the signals in NMR spectra. Therefore the final conclusion about the conformational state of C5–C6 bonds in the (1→6)-glycosidic linkages in these molecules is yet uncertain.

According to MD simulations, disaccharide fragments in the studied linear oligosaccharides were not rigid making their shapes twisted with some helical elements. The conformational shape of the cyclic di-, tri-, and tetrasaccharides was found to be symmetrical flattened ring. The larger cycles tended to adopt more complicated shapes, such as twisted rings, and the conformational behavior of their disaccharide fragments is close to that in linear oligosaccharides.

It was shown that conformational behavior of the N-acetylated compounds is similar to that of the non-N-acetylated oligoglucosamines. According to the results, the substituents at C-2 of the studied compounds protruded into the outer space and did not encounter any spatial hindrance. Hence, the introduction of N-acetyl groups did not lead to considerable conformational changes. This opens the possibility for further N-functionalization of these oligosaccharides without the loss of their spatial organization.

3. Experimental

Preparation of linear **1a,b–4a,b** and **6a,b**[7,8] and cyclic **7a,b–12a,b**[9] oligoglucosamines was described previously.

Computer simulations: Details are given in the Molecular Modeling section (**2.3.**). Transglycosidic coupling constants were calculated for each structure in the MD trajectories according to the Karplus equations and then averaged. Neural network clustering was performed in Stuttgardt Neural Network Simulator, SNNS (v. 4.2) with the use ART2 ANN. The following options were used: ART2_Weights initialization function with parameters (0.9, 2); ART2 learning function with parameters (0.95, 10, 10, 0.1, 0.9) and ART2_Stable update function with the same parameters.

The NMR spectra of oligofucosides **1a,b–4a,b** (10–15 mg) were recorded in D_2O (99.98% D, Merck, 0.5 ml) solutions on Bruker spectrometers DRX-500 and AV-600 with 0.05% acetone as reference (^1H 2.225 ppm, ^{13}C 31.45 ppm). The pH of solutions was about 5.5, the temperature was chosen so that the signal of residual protons of HOD in ^1H NMR spectra did not overlap with the signals of protons of oligoglucosamines. Thus, the spectra were acquired at the temperature of 300–310 K. Microtubes (Shigemi, Inc.) were sometimes used for sensitivity enhancement. The resonance assignment in ^1H and ^{13}C NMR spectra was performed by gradient enhanced 2D gCOSY, gNOESY, gHSQC, gJ-HMBC and gHSQC-TOCSY experiments as well as TOCSY and ROESY experiments.

Experimental $^3J_{C,H}$ constants were measured using J-HMBC[15,16] and J-resolved[17,18] techniques. The 2D J-HMBC experiment was performed in the constant-time version.[15] The spectral widths were about 2 ppm for ^1H region and 46 ppm for ^{13}C region and did not include resonances of aglycon groups. The data were collected in the echo/anti-echo mode. For echo selection the two sinusoidal field gradients in a ratio of 5:−3 were applied, and for anti-echo selection the ratio was −3:5. The length of gradients was 1 ms, and the recovery time was 100 μs. The spectra were acquired with 60–110 t_1 increments and 64–700 scans per increment. 512 points were collected during the acquisition time t_2. The HMBC preparation delay Δ for the reliable measurement of a coupling constants should be taken at least 60% of inversed values of smallest coupling of interest ($\Delta=0.6/J_{C,H}^{min}$).[16] Smaller values of Δ lead to the overestimation of J because of the antiphase character of the peaks. Δ=300 ms was used that corresponded to $J_{C,H}^{min}$=2.0 Hz. The upscaling coefficient *k* was 30–60. The relaxation delay was 1s. Thus, resulting acquisition time was 1–15 hr. The third order low-pass J-filter[16] was introduced for the suppression of one bond constants ($^1J_{C,H}$) in the range from 125 Hz to 180 Hz. Sinusoidal field gradient sequence with the ratio +7:−4:−2:−1 was applied during low-pass J-filter. The forward linear prediction to 1024 points was used in F_1 that corresponded to resolution 5–6 Hz, and zero-filling to 1024 points was used in F_2. The processing was performed with π/2 shifted sine square function in both dimensions.

J-resolved experiments were performed in direct ^{13}C-detecting mode with the PENDANTE preparation sequence for the enhancement of the sensitivity of carbon atoms. The spectral widths were about 46 ppm for ^{13}C dimensional and 14 Hz for J dimensional. The spectra were acquired with 44 t_1 increments and 500–740 scans per increment. 2048 points were collected during the acquisition time t_2 giving a spectral resolution of about 2.3 Hz in ^{13}C dimension. The relaxation time between each individual scan was 1s. The resulting acquisition time was 10–15 hr. A Gauss shaped pulse was used, its duration τ was 20–50 ms corresponding to the required selectivity of 50–20 Hz. Zero-filling to 128 points was used for the J dimension prior to Fourier transformation, giving a spectral resolution of about 0.3 Hz. The 2D spectra were processed with π/2 shifted sine square function in ^{13}C-dimension and in the J dimension.

Supplementary Material

Refer to Web version on PubMed Central for supplementary material.

Acknowledgments

We thank Dr. Yu. A. Strelenko for helpful discussions of NMR experiments. This work was supported by the grants of the President of the Russian Federation to Young Scientists MK-5544.2010.3 (A. A. Grachev) and the Russian Foundation for Basic Research 10-03-01012-a (A. G. Gerbst).

References

1. Cerca N, Jefferson KK, Maira-Litran T, Kelly-Quintos C, Goldmann DA, Azeredo J, Pier GB. Infect. Immun. 2007; 75:3406–3413. [PubMed: 17470540]
2. Itoh Y, Wang X, Hinnebusch BJ, Preston JF 3rd, Romeo T. J. Bacteriol. 2005; 187:382–387. [PubMed: 15601723]
3. Izano EA, Sadovskaya I, Vinogradov E, Mulks MH, Velllyagounder K, Ragunath C, Kher WB, Ramasubbu N, Jabbouri S, Perry MB, Kaplan JB. Microb. Pathogenesis. 2007; 43:1–9.
4. Mack D, Fischer W, Krokotsch A, Leopold K, Hartmann R, Egge H, Laufs R. J. Bacteriol. 1996; 178:175–183. [PubMed: 8550413]
5. Sloan GP, Love CF, Sukumar N, Mishra M, Deora R. J. Bacteriol. 2007; 189:8270–8276. [PubMed: 17586629]
6. Wang X, Preston JF 3rd, Romeo T. J. Bacteriol. 2004; 186:2724–2734. [PubMed: 15090514]
7. Gening ML, Tsvetkov YE, Pier GB, Nifantiev NE. Russ. J. Bioorgan. Chem. 2006; 32:389–399.
8. Gening ML, Tsvetkov YE, Pier GB, Nifantiev NE. Carbohydr. Res. 2007; 342:567–575. [PubMed: 16952342]
9. Gening ML, Titov DV, Grachev AA, Gerbst AG, Yudina ON, Shashkov AS, Chizhov AO, Tsvetkov YE, Nifantiev NE. Eur. J. Org. Chem. 2010; 13:2465–2475.
10. Gening ML, Maira-Litran T, Kropec A, Skurnik D, Grout M, Tsvetkov YE, Nifantiev NE, Pier GB. Infect. Immun. 2010; 78:764–772. [PubMed: 19948836]
11. Grachev AA, Gerbst AG, Ustyuzhanina NE, Khatuntseva EA, Shashkov AS, Usov AI, Nifantiev NE. J. Carbohydr. Chem. 2005; 24:85–100.
12. Grachev AA, Gerbst AG, Ustuzhanina NE, Krylov VB, Shashkov AS, Usov AI, Nifantiev NE. Mendeleev Commun. 2007; 17:57–62.
13. Douhal, A., editor. Chemical, Physical and Biological Aspects of Confined Systems. Vol. Volume 1. Amsterdam: Elsevier Science; 2006. Cyclodextrin Materials Photochemistry, Photophysics and Photobiology.
14. Bonas G, Vignon MR, Pérez S. Carbohydr. Res. 1991; 211:191–205. [PubMed: 1663000]
15. Gotfredsen CH, Meissner A, Duus JØ, Sørensen OW. Magn. Reson. Chem. 2000; 38:692–695.
16. Meissner A, Sørensen OW. Magn. Reson. Chem. 2001; 39:49–52.
17. Bax A, Freeman R. J. Am. Chem. Soc. 1982; 104:1099–1100.
18. Liu M, Farant RD, Gillam JM, Nicholson JK, Lindon JC. J. Magn. Reson. Series B. 1995; 109:275–283.
19. Grachev AA, Gerbst AG, Shashkov AS, Nifantiev NE. Russ. Chem. Rev. 2009; 78:717–736.
20. Olsson U, Sáwén E, Stenutz R, Widmalm G. Chem. Eur. J. 2009; 15:8886–8894.
21. Gagnaire D, Tran V, Vignon M. J. Chem. Soc. Chem. Commun. 1976; 1:6–7.
22. Gagnaire D, Vignon M. Carbohydr. Res. 1976; 51:140–144.
23. Mulloy B, Frenkiel TA, Davies DB. Carbohydr. Res. 1988; 184:39–46. [PubMed: 3242815]
24. Stenutz R, Carmichael I, Widmalm G, Serianni AS. J. Org. Chem. 2002; 67:949–958. [PubMed: 11856043]
25. Popov, AI.; Hallenga, K. Modern NMR techniques and their application in chemistry. New York: Marcel Dekker, Inc; 1991.
26. Lipkind GM, Shashkov AS, Knirel YA, Vinogradov EV, Kochetkov NK. Carbohydr. Res. 1988; 175:59–75. [PubMed: 3378242]
27. Pérez S, Imberty A, Engelsen SB, Gruza J, Mazeau K, Jimenez-Barbero J, Poveda A, Espinosa J-F, van Eyck BP, Johnson G, French AD, Kouwijzer MLCE, Grootenuis PDJ, Bernardi A, Raimondi L, Senderowitz H, Durier V, Vergoten G, Rasmussen K. Carbohydr. Res. 1998; 314:141–155.

28. Rosen J, Robobi A, Nyholm P-G. Carbohydr. Res. 2002; 337:1633–1640. [PubMed: 12423964]
29. Stortz CA. Carbohydr. Res. 1999; 322:77–86. [PubMed: 10629950]
30. Kirschner KN, Woods RJ. PNAS. 2001; 98:10541–10545. [PubMed: 11526221]
31. Carpenter GA, Grossberg S. Comput. Vision Graph. 1987; 37:54–115.
32. Grossberg S. Biol. Cybern. 1976; 23:121–134. [PubMed: 974165]
33. Grossberg S. Biol. Cybern. 1976; 23:187–202. [PubMed: 963125]
34. Najdoo KJ, Kuttel M. J. Comput. Chem. 2001; 22:445–456.

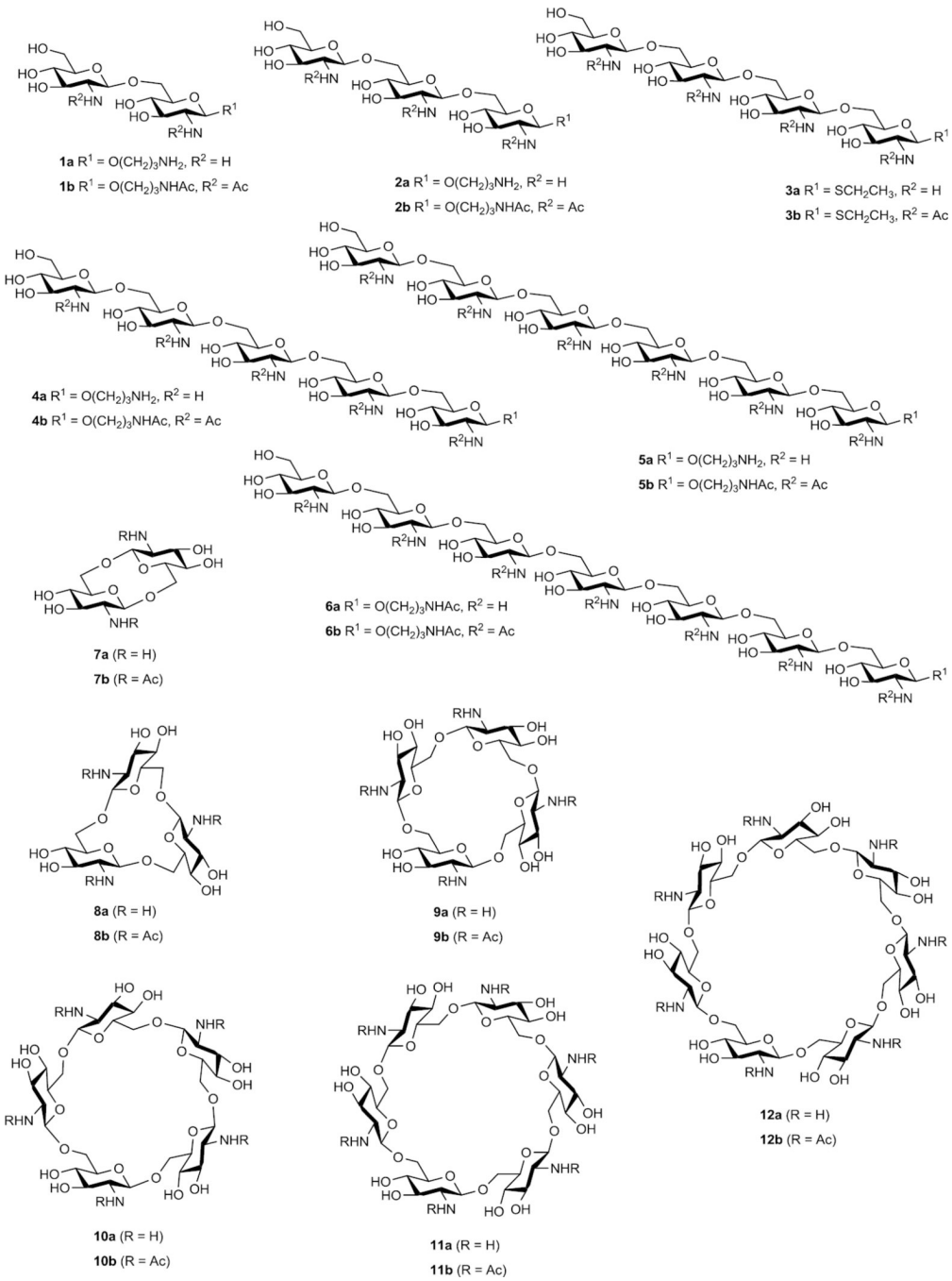

Figure 1.

Studied linear **1a,b–6a,b** and cyclic **7a,b–12a,b** oligoglucosamines. Non-N-acetylated oligosaccharides were obtained in the form of acetate salts.

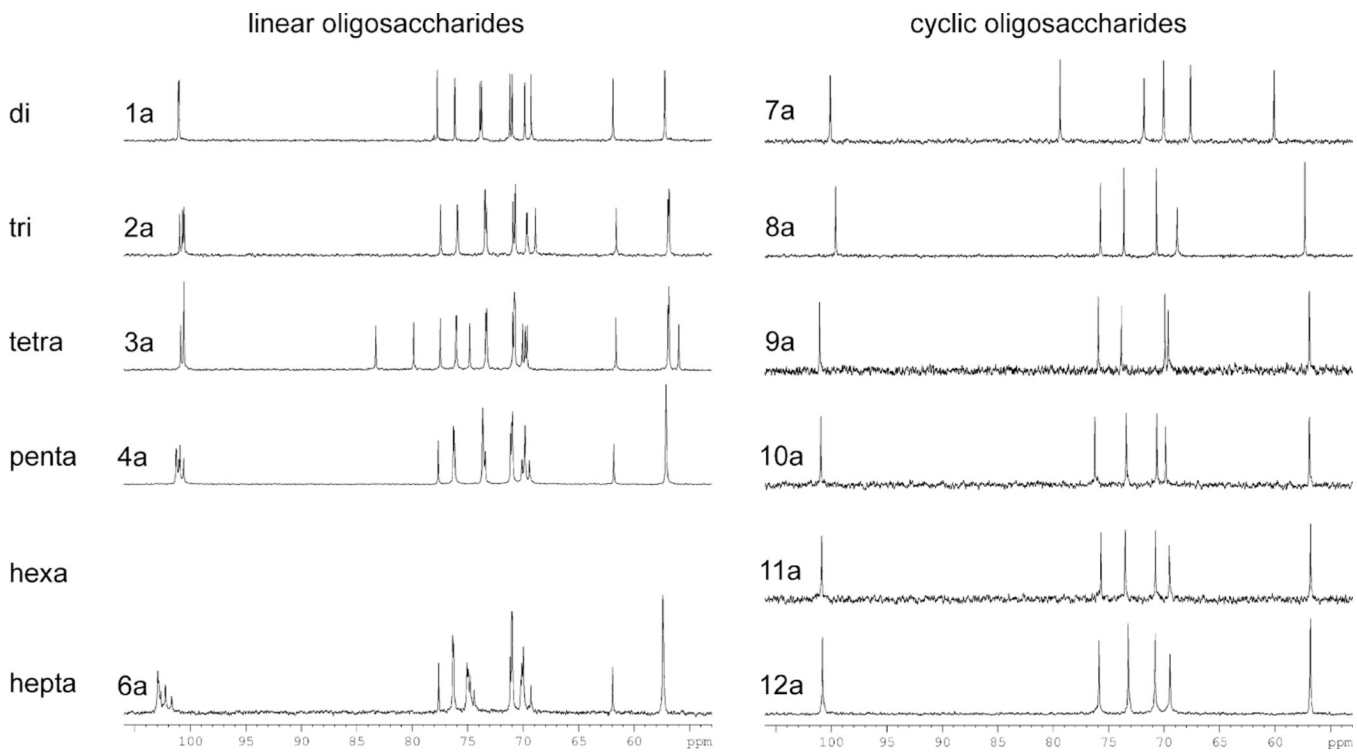

Figure 2.
^{13}C NMR spectra (carbohydrate regions) of linear **1a–4a, 6a** and cyclic **7a–12a** oligoglucosamines.

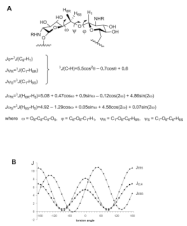

Figure 3.
Dihedral angles and the Karplus equations for the coupling constants $^{3}J_{C,H}{}^{23}$ and $^{3}J_{H,H}{}^{24}$ describing the conformation of the (1→6)-linkage (***A***) and the graphs of Karplus functions (***B***).

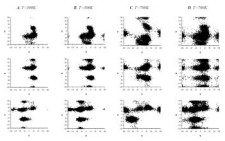

Figure 4.
Scatter plots for pairs of angles (φ, ψ**R**), (φ, ω) and (ψ**R**, ω) for internal disaccharide fragments of linear trisaccharide **2b** (***A***) and heptasaccharide **6b** (***B***) and their cyclic analogs **8b** (***C***) and **12b** (***D***). These scatter plots were built up with the use of SASA MD-simulation data at the temperature T=300 K for linear molecules **2b** and **6b** and T=700 K for cycles **8b** and **12b**.

Figure 5.
Four main conformations of (1→6)-β-linkage in the studied saccharides. Conformer **I** (φ, ψ_R, ψ_S, ω)=(40°, −140°, −25°, −60°); conformer **II**: (φ, ψ_R, ψ_S, ω)= (40°, −60°, 60°, −60°); conformer **III**: (φ, ψ_R, ψ_S, ω)= (40°, −140°, −25°, 60°); conformer **IV**: (φ, ψ_R, ψ_S, ω)= (40°, −60°, 60°, 60°).

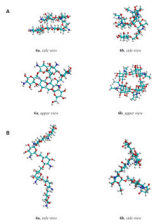

Figure 6.
The shapes corresponding to the energy minima of heptaglucosaminide **6a** and per-N-acetylated heptaglucosaminide **6b** calculated without the account of solvent effects (tending to be a right-hand helix) (***A***) and calculated with SASA solvent model (rather complicated twisted shape with some helical elements) (***B***).

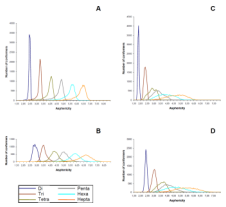

Figure 7.
Asphericity distributions calculated from SASA MD-simulations for linear oligoglucosamines **1a–6a** (***A***), linear oligo-N-acetylglucosamines **1b–6b** (***B***), cyclic oligoglucosamines **7a–12a** (***C***) and cyclic oligo-*N*-acetylglucosamines **7b–12b** (***D***).

Table 1

^{1}H NMR data[a] for linear oligosaccharides **1a,b** – **4a,b** and **6a,b** (D_2O, 500.13 or 600.13 MHz, 300–307 K[b]).

Residue	R = H								R = Ac							
	#	H-1	H-2	H-3	H-4	H-5	H-6R	H-6S	#	H-1	H-2	H-3	H-4	H-5	H-6R	H-6S
→6)-D-GlcNHR-β-aglycon[a]	**1a**	4.74	3.03	3.67	3.57	3.70	3.97	4.24	**1b**	4.48	3.65	3.52	3.38	3.55	3.73	4.2
D-GlcNHR-β-(1→		4.76	3.05	3.67	3.48	3.52	3.78	3.94		4.54	3.72	3.55	3.45	3.45	3.75	3.93
→6)-D-GlcNHR-β-aglycon[a]		4.71	3.01	3.65	3.52	3.66	3.90	4.22		4.46	3.64	3.52	3.38	3.55	3.70	4.15
→6)-D-GlcNHR-β-(1→	**2a**	4.74	3.02	3.65	3.54	3.66	3.93	4.22	**2b**	4.51	3.69	3.54	3.40	3.56	3.75	4.19
D-GlcNHR-β-(1→		4.74	3.02	3.65	3.44	3.47	3.74	3.90		4.55	3.73	3.55	3.44	3.44	3.74	3.92
→6)-D-GlcNHR-β-aglycon[a]		4.76	3.14	3.63	3.49	3.68	3.84	4.22		4.61	3.72	3.53	3.4	3.58	3.67	4.14
→6)-D-GlcNHR-β-(1→	**3a**	4.75	3.04	3.63	3.52	3.67	3.91	4.22	**3b**	4.51	3.7	3.53	3.4	3.56	3.74	4.14
→6)-D-GlcNHR-β-(1→		4.75	3.04	3.63	3.52	3.67	3.91	4.22		4.53	3.7	3.56	3.4	3.56	3.76	4.19
D-GlcNHR-β-(1→		4.74	3.03	3.65	3.46	3.48	3.74	3.90		4.54	3.73	3.55	3.45	3.45	3.75	3.92
→6)-D-GlcNHR-β-aglycon[a]		4.65	2.96	3.62	3.47	3.62	3.85	4.18		4.48	3.65	3.54	3.38	3.55	3.68	4.15
→6)-D-GlcNHR-β-(1→	**4a**	4.72	3.00	3.63	3.49	3.63	3.87	4.20	**4b**	4.52	3.70	3.55	3.40	3.56	3.75	4.17
→6)-D-GlcNHR-β-(1→		±0.01	±0.01	±0.02	±0.01	±0.02	±0.02	±0.01		±0.01			±0.01		±0.02	±0.02
→6)-D-GlcNHR-β-(1→																
D-GlcNHR-β-(1→		4.70	3.00	3.62	3.42	3.45	3.71	3.87		4.55	3.73	3.55	3.45	3.45	3.75	3.93
→6)-D-GlcNHR-β-aglycon[a]		4.62	2.92	3.58	3.50	3.64	3.88	4.24								
→[6)-D-GlcNHR-β-(1→]$_5$[c]	**6a**	4.63 ±0.02	3.00 ±0.02	3.54 ±0.02	3.49 ±0.02	3.66 ±0.02	3.88 ±0.02	4.24 ±0.02	**6b**[d]							
D-GlcNHR-β-(1→		4.67	2.93	3.58	3.48	3.48	3.76	3.93								

[a] Signals of the aglycon (in ppm): for **1a**, **2a**, **4a** OC*H*$_2$CH$_2$CH$_2$NH$_3$Ac δ 3.66–4.01; OCH$_2$C*H*$_2$CH$_2$NH$_3$Ac δ 1.82–1.98; OCH$_2$CH$_2$C*H*$_2$NH$_3$Ac δ 3.10–3.38; OCH$_2$CH$_2$CH$_2$NH$_3$*Ac* δ 1.87–1.91; for **1b**, **2b**, **4b**, **6b** and **6a** OC*H*$_2$CH$_2$CH$_2$NHAc δ 3.57–3.94; OCH$_2$C*H*$_2$CH$_2$NHAc δ 1.75–1.82; OCH$_2$CH$_2$C*H*$_2$NHAc δ 3.14–3.30; OCH$_2$CH$_2$CH$_2$NH*Ac* δ 1.97–2.05; for **3a**, **3b** SC*H*$_2$CH$_3$ δ 2.68–2.75; SCH$_2$C*H*$_3$ δ 1.23–1.25.

[b] The NMR spectra were acquired at the temperature of 300–307 K. For each compound the temperature was chosen so that to exclude the overlap of the solvent signal (HOD) with signals of the anomeric protons in ^{1}H NMR spectrum.

[c] The signals of all internal glucosamine residues.

[d] The full assignment of signals in ^{1}H and ^{13}C NMR spectra of heptasaccharide **6b** by 2D spectroscopy was not made. This compound was characterized by ^{1}H NMR and MS spectra.8

Table 2

^{13}C NMR data[a] for linear oligosaccharides **1a,b** – **4a,b** and **6a,b** (D_2O, 125.75 or 150.90 MHz, 300–307 K[b]).

Residue	R = H							R = Ac					
	#	C-1	C-2	C-3	C-4	C-5	C-6	#	C-1	C-2	C-3	C-4	C-5	C-6
→6)-D-GlcNHR-β-aglycon[a]	**1a**	101.0	57.2	73.8	71.0	76.1	69.8	**1b**	102.5	57.0	75.2	71.4	76.0	70.0
D-GlcNHR-β-(1→		101.0	57.2	73.7	71.2	77.7	61.8		102.9	57.0	75.2	71.4	77.3	62.2
→6)-D-GlcNHR-β-Agl[a]		100.5	56.9	73.3	70.7	76.0[e]	69.6[f]		102.5	57.0	75.2[g]	71.4	75.9	69.9
→6)-D-GlcNHR-β-(1→	**2a**	101.0	56.9	73.4	70.7	75.9[e]	69.7[f]	**2b**	102.9	57.0	75.2[g]	71.4	76.1	69.9
D-GlcNHR-β-(1→		100.7	56.9	73.4	70.9	77.4	61.6		102.9	57.0	75.3[g]	71.4	77.3	62.2
→6)-D-GlcNHR-β-Ag1[a]		83.3	56.0	74.8	70.8	79.9	70.1		85.4	56.2	76.7	71.4	79.9	70.1
→6)-D-GlcNHR-β-(1→	**3a**	100.6	56.9	73.3	70.8	76.0[g]	69.8	**3b**	102.8	56.9	75.3	71.4	76.1	69.9
→6)-D-GlcNHR-β-(1→		100.9	56.9	73.3	70.8	76. 1[g]	69.6		103	56.9	75.2	71.4	76.1	70
D-GlcNHR-β-(1→		100.6	56.9	73.4	70.9	77.5	61.6		103	57.0	75.2	71.4	77.3	62.2
→6)-D-GlcNHR-β-Agl[a]		100.6	57.1	73.4	71.0	76.2	69.8		102.5	56.9	75.2	71.5	76.1	69.9
→6)-D-GlcNHR-β-(1→														
→6)-D-GlcNHR-β-(1→	**4a**	101.1 ±0.2	57.1	73.6	71.0	76.3 ±0.1	69.9 ±0.1	**4b**	103.0 ±0.1	56.9	75.2	71.5 ±0.1	76.0	70.0 ±0.1
→6)-D-GlcNHR-β-(1→														
D-GlcNHR-β-(1→		100.9	57.1	73.6	71.1	77.6	61.8		102.9	56.9	75.2	71.4	77.3	62.2
→6)-D-GlcNHR-β-Agl[a]		101.7	57.4	74.4	71.0	76.3	70.0							
→[6)-D-GlcNHR-β-(1→]$_5$[c]	**6a**	102.8 ±0.1	57.1	75.0 ±0.1	71.0	76.3 ±0.1	70.1 ±0.1	**6b**[d]						
D-GlcNHR-β-(1→		102.3	57.4	74.8	71.2	77.6	61.9							

[a] Signals of the aglycon (in ppm): for **1a**, **2a**, **4a** O$\underline{C}$H$_2$CH$_2$CH$_2$NH$_3$Ac δ 68.9–69.4; OCH$_2\underline{C}$H$_2$CH$_2$NH$_3$Ac δ 27.9–30.0; OCH$_2$CH$_2\underline{C}$H$_2$NH$_3$Ac δ 37.4–38.4; OCH$_2$CH$_2$CH$_2$NH$_3\underline{Ac}$ δ 24.2–24.7; for **1b**, **2b**, **4b**, and **6a** O$\underline{C}$H$_2$CH$_2$CH$_2$NHAc δ 69.1–69.3; OCH$_2\underline{C}$H$_2$CH$_2$NHAc δ 29.6–29.9; OCH$_2$CH$_2\underline{C}$H$_2$NHAc δ 37.6–37.8; OCH$_2$CH$_2$CH$_2$NH$\underline{Ac}$ δ 23.3–23.8; and 175.6–175.9; for **3a**, **3b** S$\underline{C}$H$_2$CH$_3$ δ 25.9; SCH$_2\underline{CH_3}$ δ 15.8.

[b] The NMR spectra were acquired at the temperature of 300–307 K. For each compound the temperature was chosen so that to exclude the overlap of the solvent signal (HOD) with signals of the anomeric protons in ^{1}H NMR spectrum.

[c] The signals of all internal glucosamine residues.

[d] The full assignment of signals in ^{1}H and ^{13}C NMR spectra of heptasaccharide **6b** by 2D spectroscopy was not made. This compound was characterized by ^{1}H NMR and MS spectra.[8]

e, f, g The assignment may be reversed.

Table 3

^{1}H NMR data[a] for cyclic oligosaccharides **7a** – 12**b** (D_2O, 500.13 or 600.13 MHz, 303–310 K[b]).[9]

Residue	R = H·								R = Ac							
	#	H-1	H-2	H-3	H-4	H-5	H-6R	H-6S	#	H-1	H-2	H-3	H-4	H-5	H-6R	H-6S
→6)-D-GlcNHR-β-(1→	**7a**	4.95	3.33	3.72	4.17	3.85	3.73	4.12	**7b**	4.68	3.94	3.62	4.32	3.72	4.17	3.61
→6)-D-GlcNHR-β-(1→	**8a**	4.79	3.03	3.65	3.56	3.56	4.01	4.22	**8b**	4.60	3.64	3.49	3.46	3.48	4.09	3.90
→6)-D-GlcNHR-β-(1→	**9a**	4.74	3.03	3.67	3.72	3.60	4.07	4.14	**9b**	4.57	3.67	3.53	3.52	3.51	3.94	4.02
→6)-D-GlcNHR-β-(1→	**10a**	4.77	3.04	3.65	3.58	3.61	4.03	4.13	**10b**	4.59	3.67	3.55	3.46	3.53	3.90	4.07
→6)-D-GlcNHR-β-(1→	**11a**	4.73	3.02	3.64	3.55	3.68	3.97	4.21	**11b**	4.54	3.63	3.59	3.40	3.54	3.77	4.10
→6)-D-GlcNHR-β-(1→	**12a**	4.79	3.06	3.67	3.60	3.66	3.96	4.20	**12b**	4.58	3.70	3.57	3.47	3.57	3.82	4.13

[a] Signal of the Ac^- δ1.90–1.91 for **7a–12a**; signal of the Ac δ 2.02–2.05 for **7b-12b**.

[b] The NMR spectra were acquired at the temperature of 303–310 K. For each compound the temperature was chosen so that to exclude the overlap of the solvent signal (HOD) with signals of the anomeric protons in ^{1}H NMR spectrum.

Table 4

^{13}C NMR[a] data for cyclic oligosaccharides **7a** – 12**b** (D_2O, 125.75 or 150.90 MHz, 303–310 K[b]).[9]

Residue	R = H							R = Ac						
	#	C-1	C-2	C-3	C-4	C-5	C-6	#	C-1	C-2	C-3	C-4	C-5	C-6
→6)-D-GlcNHR-β-(1→	**7a**	100.1	60.1	71.8	67.6	79.4	70.0	**7b**	103.3	59.9	74.3	67.9	78.1	71.3
→6)-D-GlcNHR-β-(1→	**8a**	99.6	57.3	73.6	70.7	75.7	68.8	**8b**	101.4	57.0	75.2	70.6	75.8	69.7
→6)-D-GlcNHR-β-(1→	**9a**	100.5	56.9	73.4	70.1	76.0	69.7	**9B**	102.3	56.7	75.0	70.5	75.9	69.5
→6)-D-GlcNHR-β-(1→	**10a**	100.9	56.9	73.4	70.6	76.2	69.8	**10b**	102.8	56.8	74.8	71.0	76.2	69.9
→6)-D-GlcNHR-β-(1→	**11a**	100.8	56.8	73.5	70.8	75.7	69.5	**11b**	102.6	56.9	74.7	71.3	75.7	70.2
→6)-D-GlcNHR-β-(1→	**12a**	100.8	56.8	73.2	70.8	75.9	69.5	**12b**	102.7	56.8	74.9	71.3	75.9	69.8

[a] Signal of the Ac^- δ24.0–24.6 and 181.8–182.7 for **7a–12a**; signal of the Ac δ 23.3–23.6 and 175.6–175.9 for **7b-12b**.

[b] The NMR spectra were acquired at the temperature of 303–310 K. For each compound the temperature was chosen so that to exclude the overlap of the solvent signal (HOD) with signals of the anomeric protons in ^{1}H NMR spectrum.

Table 5

Experimental[a] and calculated values of transglycosidic ^3J (Hz) coupling constants (Fig. 3) for middle units[b] of linear oligoglucosamines **1a–6b**.

Method	*Non-N-acetylated oligoglucosamines*						*N-acetylated oligoglucosamines*					
	#	Jφ	JψR	JψS	JωS	JωS	#	Jφ	JψR	JψS	JωR	JωS
experiment		**3.0**	**2.9**	**3.0**	**5.0**	**2.0**[g]		**4.2**	**2.8**	**3.1**	**6.1**	**1.9**[g]
calc.[c](ε = 81)	**1a**	3.4	2.3	2.3	8.5	3.1	**1b**	3.3	2.2	2.0	2.3	1.9
calc.[d](SASA)		3,6	1,8	2,1	9,4	1,6		3.7	2.7	2.3	6.8	1.7
calc.[e] (NH_3)		3.4	2.3	2.3	6.6	2.2						
experiment		**3.5**	**3.0**	**2.3**	[f]	**2.0**[g]		**4.3**	**3.0**	**2.9**	[f]	**2.1**[g]
calc. (ε = 81)	**2a**	3.3	2.3	2.3	6.7	2.4	**2b**	3.4	2.4	2.1	6.4	3.5
calc. (SASA)		3,7	2,1	2,1	9,4	1,8		3.1	2.3	2.1	3.6	2.2
calc. (NH_3)		3.4	2.0	2.3	5.4	2.3						
experiment		**3.8**	**2.9**	**2.8**	[f]	**2.0**[g]		**4.2**	**2.7**	**2.6**	[f]	**2.0**[g]
calc. (ε = 81)	**3a**	3.3	2.4	2.6	5.5	2.0	**3b**	3.5	3.1	2.9	7.9	1.9
calc. (SASA)		3,9	2,0	2,3	8,4	3,0		3.1	2.5	2.0	4.8	1.7
calc. (NH_3)		3.3	2.4	2.5	6.2	2.0						
experiment		[f]	[f]	[f]	[f]	[f]		≈**3.8**[h]	≈**2.9**[h]	≈**2.7**[h]	[f]	**2.0**[g]
calc. (ε = 81)	**4a**	3.2	2.8	2.4	5.8	2.1	**4b**	3.4	2.6	2.4	4.4	2.2
calc. (SASA)		3,5	2,2	2,1	6,1	2,7		3.1	2.7	1.9	7.2	1.8
calc. (NH_3)		3.3	2.6	2.3	5.0	2.0						
experiment		[j]	[j]	[j]	[j]	[j]		[j]	[j]	[j]	[j]	[j]
calc. (ε = 81)	**5a**	3.3	2.9	2.6	6.3	2.7	**5b**	3.3	2.5	2.2	3.7	2.0
calc. (SASA)		3,5	2,3	2,0	6,1	2,5		3.3	2.7	2.1	7.7	1.8
calc. (NH_3)		3.2	2.1	2.4	4.1	3.5						
experiment		[f]	[f]	[f]	[f]	[f]		[f]	[f]	[f]	[f]	[f]
calc. (ε = 81)	**6a**	3.4	2.7	2.7	4.4	2.1	**6b**	3.4	3.2	2.8	6.4	2.7

Method	*Non-N-acetylated oligoglucosamines*						*N-acetylated oligoglucosamines*					
	#	**Jφ**	**JψR**	**JψS**	**JωS**	**JωS**	#	**Jφ**	**JψR**	**JψS**	**JωR**	**JωS**
calc. (SASA)		3,7	2,2	2,1	7,0	2,5		3.2	2.6	1.8	5.3	2.1
calc. (NH_3)		3.2	2.4	2.4	6.8	2.2						

[a]The NMR spectra were acquired at the temperature of 300–307 K. For each compound the temperature was chosen so that to exclude the overlap of the solvent signal (HOD) with signals of the anomeric protons in ^{1}H NMR spectrum.

[b]The data for all disaccharide units of oligoglucosamines are presented in Supplementary Materials.

[c]The values of constants calculated for solvation model ε = 81 at TE = 300K.

[d]The values of constants calculated for SASA implicit solvation model at TE = 300K.

[e]The values of constants calculated for NH3-model of free oligoglucosamines **1a–6a** at ε = 81 and TE = 300K.

[f]Not determined due to the peak overlaps.

[g]The value of constant was obtained by the curve-fitting algorithm[25] which was applied for analysis of multiplet due to the small value of the interesting constant and the broad lines in multiplet.

[h]The value of the coupling constant could not be measured exactly because the peaks overlap in the spectra.

[j]Not measured.

Carbohydr Res. Author manuscript; available in PMC 2012 November 8.

Table 6

Experimental[a] and averaged calculated[b] values of transglycosidic ^3J (Hz) coupling constants (Fig. 3) for cyclic oligoglucosamines **7a – 12b**.

Method	*Non-N-acetylated oligoglucosamines*						*N-acetylated oligoglucosamines*					
	#	Jφ	JψR	JψS	JωR	JωS	#	Jφ	JψR	JψS	JψR	JψS
experiment		**4.3**	**2.2**	**6.0**	**2.6**[g]	**≈1.0**[h]		**3.4**	**2.3**	**6.4**	**2.4**[g]	*-*[f]
calc.[c](ε = 81)	**7a**	4.7	4.1	4.4	5.4	1.6	**7b**	4.8	4.0	4.5	5.1	1.4
calc.[d](SASA)		4.8	4.1	4.4	5.4	1.5		4.4	3.8	3.9	5.3	1.6
calc.[e] (NH_3)		4.6	3.8	4.3	5.0	1.5						
experiment		**3.4**	**2.3**	**6.5**	**2.1**[g]	**0.9**[g]		**3.7**	**2.7**	**6.1**	**4.1**[g]	**1.4**[g]
calc. (ε = 81)	**8a**	3.4	1.5	4.1	2.2	1.7	**8b**	3.4	1.6	4.1	2.3	1.7
calc. (SASA)		3.5	2.1	4.1	3.3	1.6		3.6	2.4	4.0	3.7	1.8
calc. (NH_3)		3.5	1.5	4.1	2.3	1.7						
experiment		**4.4**	**2.3**	**2.4**	**3.0**	**1.6**[g]		**4.8**	**2.5**	**3.2**	**2.7**[g]	**1.2**[g]
calc. (ε = 81)	**9a**	3.8	2.3	2.7	3.5	2.0	**9b**	3.7	2.3	2.8	3.5	2.1
calc. (SASA)		3.9	2.4	2.8	4.2	2.0		3.8	2.6	2.9	4.5	2.2
calc. (NH_3)		3.8	1.5	3.2	2.5	1.5						
experiment		**3.8**	**2.7**	**2.8**	**4.0**	**1.7**[g]		**4.4**	**3.6**	**2.8**	**4.9**	**1.8**[g]
calc. (ε = 81)	**10a**	3.5	2.8	2.8	5.0	3.2	**10b**	3.5	2.7	2.8	4.9	3.4
calc. (SASA)		3.6	2.7	2.7	4.9	3.2		3.6	2.8	2.8	5.0	3.0
calc. (NH_3)		3.5	2.7	2.8	5.0	3.5						
experiment		**3.9**	**3.9**	**2.5**	**4.9**	**2.1**[g]		**3.5**	**3.8**	**2.4**	**6.0**	**1.9**[g]
calc. (ε = 81)	**11a**	3.5	2.7	2.7	5.2	3.4	**11b**	3.4	2.6	2.6	4.8	3.5
calc. (SASA)		3.5	2.7	2.6	4.7	3.3		3.5	2.8	2.6	4.8	3.0
calc. (NH_3)		3.5	2.7	2.6	5.0	3.6						
experiment		**3.8**	**3.5**	**3.2**	**4.0**	**2.0**[g]		**3.9**	**3.5**	**2.8**	**5.2**	**2.0**[g]
calc. (ε = 81)	**12a**	3.5	2.7	2.7	5.5	3.4	**12b**	3.4	2.6	2.6	5.1	3.5

Method	*Non-N-acetylated oligoglucosamines*						*N-acetylated oligoglucosamines*					
	#	**Jφ**	**JψR**	**JψS**	**JωR**	**JωS**	#	**Jφ**	**JψR**	**JψS**	**JψR**	**JψS**
calc. (SASA)		3.5	2.7	2.5	4.9	3.4		3.5	2.7	2.5	4.9	3.1
calc. (NH_3)		3.5	2.6	2.6	5.3	3.5						

[a]The NMR spectra were acquired at the temperature of 300–307 K. For each compound the temperature was chosen so that to exclude the overlap of the solvent signal (HOD) with signals of the anomeric protons in ^{1}H NMR spectrum.

[b]The calculated values for every disaccharide units of oligoglucosamines are presented in Supplementary Materials.

[c]The values of constants calculated for solvation model ε = 81 at TE = 700K.

[d]The values of constants calculated for SASA implicit solvation model at TE = 700K.

[e]The values of constants calculated for NH3-model of free oligoglucosamines **7a–12a** at ε = 81 and TE = 700K.

[f]Not determined due to the peak overlaps.

[g]The value of constant was obtained by the curve-fitting algorithm[25] which was applied for analysis of multiplet due to the small value of the interesting constant and the broad lines in multiplet.

[h]The value of the coupling constant could not be measured exactly because the peaks overlap in the spectra.

Carbohydr Res. Author manuscript; available in PMC 2012 November 8.